Flat-band conductivity properties at long-range Coulomb interactions

Wolfgang Häusler

Angaben zur Veröffentlichung / Publication details:

Häusler, Wolfgang. 2015. "Flat-band conductivity properties at long-range Coulomb interactions." *Physical Review B* 91 (4): 041102(R).
https://doi.org/10.1103/physrevb.91.041102.

PHYSICAL REVIEW B **91**, 041102(R) (2015)

Flat-band conductivity properties at long-range Coulomb interactions

Wolfgang Häusler
Institut für Physik, Universität Augsburg, D-86135 Augsburg, Germany
and I. Institut für Theoretische Physik, Universität Hamburg, D-20355 Hamburg, Germany
(Received 1 August 2014; revised manuscript received 12 December 2014; published 6 January 2015)

Dispersionless (flat) electronic bands are investigated regarding their conductance properties. Due to "caging" of carriers these bands are usually insulating at partial filling, at least on a noninteracting level. Considering the specific example of a $\mathcal{T}_3$ lattice, we study long-range Coulomb interactions. A nontrivial dependence of the conductivity on flat-band filling is obtained, exhibiting an infinite number of zeros. Near these zeros, the conductivity rises linearly with carrier density. At densities halfway in between adjacent conductivity zeros, strongly enhanced conductivity is predicted, accompanying a solid-solid phase transition.

DOI: 10.1103/PhysRevB.91.041102 PACS number(s): 73.20.Jc, 71.10.Fd, 73.20.Qt

Recently, electronic flat bands in periodic lattices have received considerable attention [1], where single particle energies ε_k of at least one tight binding band stay nondispersing or weakly dispersing throughout the Brillouin zone. One focus of interest in two spatial dimensions, similar to Landau levels, is the effect of interactions which in the absence of kinetic energy always has to be treated nonperturbatively. Fractional Chern insulator phases have been identified in almost flat bands [2,3], some of which exhibit Chern numbers larger than unity [4] and thereby generalize fractional quantum Hall states. Meanwhile, many lattices have been detected to host flat bands. Band flatness [5] arises due to localization by local quantum interferences, coined [6] as the "caging" of carriers. As a result, the conductivity vanishes, at least on a noninteracting level. This accords with the vanishing Chern number of *strictly* flat single particle bands where $d\varepsilon_k/dk = 0$, throughout the Brillouin zone, as proven recently [7] for tight binding lattices.

The on-site Hubbard interaction seems to delocalize vicinally caged carriers, which was considered as an indication of nonzero conductivity [8]. However, short-range interactions cannot impair the huge flat-band degeneracy at low fillings [9]. Competing charge density wave phases have been studied [3]. Here, we investigate long-range Coulomb interactions which at any filling will lift the flat-band degeneracy. In quantum Hall systems, when kinetic energy is quenched, they cause Wigner crystallization at fillings $\nu < \frac{1}{5}$ [10] (in graphene at $\nu < 0.28$ [11]) while, without a magnetic field, crystallization appears when the Coulomb energy E_C exceeds the kinetic energy E_K by a sufficiently large factor [12] $E_C/E_K > 37$. The longitudinal conductivity

$$\sigma(\omega) = D\frac{1}{i\omega} \tag{1}$$

of clean systems at zero temperature diverges at zero frequency ω [13] and is then due to sliding of the hexagonal crystal as a whole [14]. Its Drude weight $D = e^2n/m$ is determined by carrier density n and particle masses m, just as in the absence of interactions [15], and e is the elementary charge. We do not consider crystalline disorder here. In flat bands, where no kinetic energy competes, we always expect a Wigner crystallized phase. Conductance properties, quantified again by the Drude weight D, cannot simply be proportional to m^{-1} since m is *a priori* meaningless to parametrize kinetic energy [5]. In this Rapid Communication we determine D of flat bands in the presence of (static) Coulomb interactions. Our main result is sketched below in Fig. 2: D exhibits an infinite number of zeros at inverse band fillings [cf. Eq. (3)]. Near these zeros, the Drude weight rises linearly with the slopes that we estimate. Right in the middle, between adjacent insulating fillings, phase transitions occur for which we expect strongly enhanced conductivities.

We analyze flat bands in two dimensions exemplarily for the $\mathcal{T}_3$ lattice [6], which in literature also is called the Sutherland—or dice lattice, and which, in principle, can be realized on the basis of cold quantum gases [16,17]. It consists of three different sublattices (A, H, B), where the A and B sites are not directly connected, but only connect through the H sites (cf. Fig. 1).

With electron operators c_i^+ acting at lattice sites i we consider the model

$$H = -t\sum_{\langle i,j\rangle} c_i^+ c_j, \tag{2}$$

where hopping takes place only along the bonds $\langle i,j\rangle$, indicated in Fig. 1 as lines of lengths a. The eigenvalues ε_k of H in k-space closely resemble the band structure of graphene, with two Dirac points at the corners of the hexagonal Brillouin zone and conelike linearly dispersing bands in their vicinity. Additionally, at zero energy, there is a flat band extending throughout the Brillouin zone. In direct generalization to graphene, the long wavelength Hamiltonian near one of the two inequivalent Dirac points can be described in spinor form as $v_F\, \boldsymbol{p}\cdot\boldsymbol{S}$ when using spin-1 operators $\boldsymbol{S} = (S_x, S_y)$ [16,18] (instead of spin-$\frac{1}{2}$ operators as for graphene) to describe pseudospins that now encode the amplitudes on the three sublattices (A, H, B), with $v_F = 3ta/\sqrt{2}$ the Fermi velocity. Near the Dirac points, the carrier momentum $\boldsymbol{p}$ formally serves as the quantization axes for three pseudospin eigenstates of energies $\varepsilon_k^{(1,0,-1)} = (v_F|k|, 0, -v_F|k|)$. Here, we focus on the flat band $\varepsilon_k^{(0)} = 0$ with corresponding eigenstates $\psi_k^{(0)} = (-|k|e^{-i\varphi}, 0, |k|e^{i\varphi})/\mathcal{N}_k$ that manifest the nonpopulated central H sites ($|k|$ and $\varphi = \arctan k_y/k_x$ denote, respectively, the modulus and direction of the carrier wave vector, and $\mathcal{N}_k$ is a normalization). A small spin-orbit term consisting of intrinsic and Rashba contributions [19] removes the Dirac point by opening a gap [20] which perturbatively renormalizes

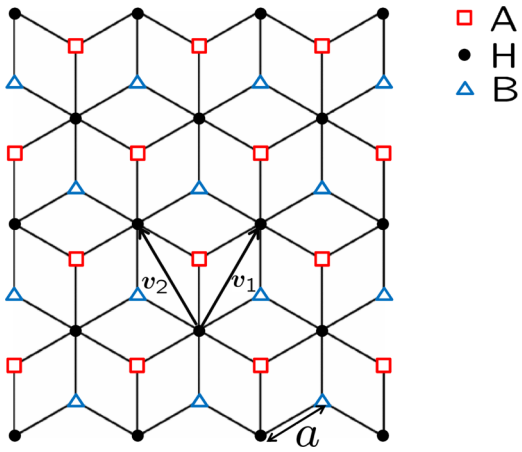

FIG. 1. (Color online) Structure of the $\mathcal{T}_3$ lattice: A (□) and B (△) sites are connected to only three nearest H (●) sites, while, conversely, H sites are sixfold coordinated. The structure implies equal numbers of lattice sites, $N_A = N_H = N_B$. $\boldsymbol{v}_1 = \frac{1}{2}(\sqrt{3},3)a$ and $\boldsymbol{v}_2 = \frac{1}{2}(-\sqrt{3},3)a$ mark the basis vectors of the $\mathcal{T}_3$ lattice, and a is the hopping distance.

to increasing values in the simultaneous presence of Coulomb interactions [19,20]; this isolates the flat band and, for small spin-orbit coupling strength, leaves $\psi_k^{(0)}$ essentially unaffected.

Linear combinations within the $(N/3)$-fold degenerate space of flat-band Bloch states ($N = N_A + N_H + N_B$ is the total number of lattice sites) allow one to construct strictly localized states around any H site, such that the entire amplitude resides on just one ring of the six nearest A and B sites surrounding a given H site, of equal magnitude but of alternating signs on the A and B sites around the ring, and vanishes elsewhere. This describes the spatial localization of "caged" quantum states in a strictly periodic lattice [21]. At fillings $\nu = 3N_e^{(0)}/N \leqslant 1$ of the flat band, only νN_H out of all rings are occupied, with $N_e^{(0)}$ the flat-band carrier number.

Long-range Coulomb interactions $\sim e^2/\kappa|\boldsymbol{r} - \boldsymbol{r}'|$ will lift the huge flat-band degeneracy by favoring maximum distances between the carriers, where κ is the dielectric constant. On a continuous space the ground state would be a Wigner crystal [22] of lattice constant $b = \sqrt{3/\nu}a = \sqrt{2/\sqrt{3}n_e}$, where a is the $\mathcal{T}_3$-lattice constant and $n_e = 2/\sqrt{3}b^2$ the flat-band carrier density. Here, however, carriers cannot occupy arbitrary continuous positions but must reside at H sites (more precisely, on rings surrounding H sites), which constrains the possible carrier positions to the hexagonal H lattice of lattice constant $\sqrt{3}a$ with which b is, in general, incommensurate at arbitrary ν. At commensurability, the basis vectors $\boldsymbol{b}$ of the Wigner lattice are integer linear combinations of the basis vectors $\boldsymbol{v}_1$ and $\boldsymbol{v}_2$ spanning the $\mathcal{T}_3$ lattice (cf. Fig. 1), $\boldsymbol{b} = n_1\boldsymbol{v}_1 + n_2\boldsymbol{v}_2$. For the magnitude $b = |\boldsymbol{b}|$ this necessitates [23]

$$\frac{b}{\sqrt{3}a} = 1/\sqrt{\nu_{n_1n_2}} \equiv \sqrt{n_1^2 + n_2^2 + n_1n_2}, \quad n_1,n_2 \in \mathbb{Z}, \quad (3)$$

for some pair of integers (n_1,n_2). Table I lists some typical examples for $\nu_{n_1n_2}^{-1} = n_1^2 + n_2^2 + n_1n_2$ satisfying (3). At these commensurate fillings $\nu_{n_1n_2}$ the conductivity vanishes, as demonstrated below. We remark that seemingly random distances $\sim\Delta_{n_1n_2}$ separate adjacent inverse commensurate fillings, with larger $\Delta_{n_1n_2}$ occurring only rarer. This is somewhat similar to prime numbers though, at the moment, we are unable to estimate the asymptotic decay for the occurrence of large $\Delta_{n_1n_2}$ as a function of the magnitude of $\Delta_{n_1n_2}$.

TABLE I. Some values of inverse commensurate fillings $\nu_{n_1n_2}^{-1} = n_1^2 + n_2^2 + n_1n_2$ satisfying (3), where (n_1,n_2) is one out of, in general, 12 pairs of associated integers. The angles $\theta_{n_1n_2} = \arctan\sqrt{3}/(1 + 2n_1/n_2)$ in degrees (chosen here as $0 \leqslant \theta_{n_1n_2} \leqslant 30°$) describe how the corresponding Wigner crystal is oriented with regard to the $\mathcal{T}_3$ lattice. Differences separating adjacent $\nu_{n_1n_2}^{-1}$ are called $\Delta_{n_1n_2}$.

$1/\nu_{n_1n_2}$	n_1	n_2	$\theta_{n_1n_2}$	$\Delta_{n_1n_2}$
3	1	1	30.	1
4	2	0	0.	3
7	2	1	19.1066	2
9	3	0	0.	3
12	2	2	30.	1
13	3	1	13.8979	3
16	4	0	0.	3
19	3	2	23.4132	2
21	4	1	10.8934	4
25	5	0	0.	2
⋮				
1477	31	12	15.6886	6
1483	38	1	1.2886	5
1488	28	16	21.0517	1
1489	37	3	3.8606	3
1492	34	8	10.3327	5
1497	32	11	14.2536	4
1501	36	5	6.4171	15
1516	30	14	18.1432	3
1519	35	7	8.9483	2
1521	39	0	0.	3
⋮				

Wigner crystallization spontaneously breaks translational and rotational symmetries so that the ensuing crystal at $\nu = \nu_{n_1n_2}$ will be oriented at angle $0 \leqslant \theta_{n_1n_2} \leqslant \pi/6$ with regard to the underlying $\mathcal{T}_3$ lattice, where $\tan\theta_{n_1n_2} = \sqrt{3}/(1 + 2n_1/n_2) = \tan(\pi/3 - \theta_{n_2n_1})$. Accounting additionally for the trivial hexagonal symmetry, $\theta_{n_1n_2} \to \theta_{n_1n_2} + n\pi/3$ for $n = 1,\ldots,5$, there are altogether at least 12 pairs of integers (n_1,n_2) characterizing commensurate Wigner lattices at the same flat-band carrier density [24]. As a result, the crystals of adjacent commensurate densities will be more or less randomly oriented (cf. Table I).

How does the ground state appear at fillings $\nu = \nu_{n_1n_2} + \delta\nu$ for $|\delta\nu| \ll \nu^2$ slightly deviating from commensurate values $\nu_{n_1n_2}$? To accommodate additional ($\delta\nu > 0$) or missing ($\delta\nu < 0$) carriers the system has basically two options: (i) Develop two domains out of two adjacent commensurate fillings each [25], or (ii) accommodate, as a $\nu_{n_1n_2}$-Wigner crystal, $\delta\nu N_H$ additional "electrons" at interstitial places or leave $\delta\nu N_H$ vacant Wigner sites as "holes," depending on the sign of $\delta\nu$. A simple energetic estimate supports the more homogeneous ground state (ii) near the commensurate fillings since domains would suffer energetically from additional charging, dipolar, and surface contributions.

For conductance properties we analyze the current density

$$\boldsymbol{j} = ev_{\mathrm{F}}\boldsymbol{S}, \tag{4}$$

which for $\mathcal{T}_3$ resembles the relativistic expression for the operator $\boldsymbol{j}$ of graphene [13,26]. In $\mathcal{T}_3$, the spin matrices

$$S_x = \frac{1}{\sqrt{2}}\begin{pmatrix} 0 & 1 & 0 \\ 1 & 0 & 1 \\ 0 & 1 & 0 \end{pmatrix}, \quad S_y = \frac{1}{\sqrt{2}}\begin{pmatrix} 0 & -i & 0 \\ i & 0 & -i \\ 0 & i & 0 \end{pmatrix} \tag{5}$$

generalize the Pauli matrices. We see that the matrix elements $\langle\psi_k^{(0)}|\boldsymbol{j}|\psi_{k'}^{(0)}\rangle$ vanish identically inside the flat band, as a result of vanishing H occupancy. As a consequence, the system is insulating since the conductivity is proportional to squares of these matrix elements, in accordance with the above caging argument. Finite conductivity necessitates finite amplitudes on H sites which, in turn, requires one to destroy the destructive quantum interference responsible for caging on the hexagonal rings surrounding the H sites, for example, by impairing the precise balance in the occupation probabilities of the A and B sites of one particular cage ring through asymmetric electrostatic forces induced by proximate charges.

For commensurate crystals, the entire environs of each Wigner site are hexagonally symmetric for any (n_1,n_2). While electrostatic forces created by vicinal Wigner sites will act on all six A and B sites encircling a given Wigner site, enhancing, e.g., their on-site potential energies, and the magnitudes of the respective hoppings t_{A} and t_{B} to the nearest H sites, no *difference* between A and B arises, $t_{\mathrm{A}} = t_{\mathrm{B}}$, thus leaving the caging intact. Therefore, at fillings $\nu = \nu_{n_1n_2}$, the flat band stays insulating in the presence of long-range Coulomb interactions.

The situation can change at fillings $\nu = \nu_{n_1n_2} + \delta\nu$. In the following we focus on low flat-band fillings $\nu \ll 1$ such that $b \gg a$ [cf. (3)]. While both types of "dopants," electrons and holes, may distort the crystal in their vicinity (however, at most by discrete displacements, constrained to H sites—we do not consider elastic distortion of the underlying $\mathcal{T}_3$ lattice here, having in mind, for example, optical lattices) to relax local electrostatic strain, this effect will have a minor impact on the conductivity, and is therefore neglected in the following. Energetically, interstitials prefer positions right in the middle of the Wigner triangles, at distances $b/\sqrt{3}$ to the nearest Wigner sites, while vacancies are merely unoccupied Wigner sites.

Generally, the electrons as well as each of the six Wigner sites next to the holes experience non-hexagonally-symmetric environs, which may mobilize them. Electrostatic forces acting *differently* on the A and B sublattices are crucial for the emerging A-B imbalance. The nearest electrostatic centers located on the perpendicular bisectors of the A and B sites still do *not* achieve such an imbalance, albeit now $t_{\mathrm{A,B}}$'s may vary in magnitude as we go around the six sites of an occupied ring while the mirror symmetry remains preserved. This kind of symmetry occurs when $\theta_{n_1n_2} = \pi/6$ for $\delta\nu > 0$ (electrons) and $\theta_{n_1n_2} = 0, \pi/3$ for $\delta\nu < 0$ (holes). As a result, near fillings $\nu_{n_1n_2}$ where $\theta_{n_1n_2} = \{^{\pi/6}_{0\ \mathrm{or}\ \pi/3}\}$, we expect vanishing conductance, yet over a finite interval $\nu = \nu_{n_1n_2} \pm |\delta\nu|$.

At all other fillings $\nu = \nu_{n_1n_2} + \delta\nu$ (with $\delta\nu \neq 0$), destructive quantum interference and local topological localization of the dopants is destroyed, H sites acquire a nonzero amplitude, and a finite delocalizing kinetic energy arises (which then has to compete with the Coulomb energy as in the ordinary Wigner transition). In principle, this allows dopants to spread across the entire $\mathcal{T}_3$ lattice, resulting in finite conductivity. To quantify the potential *difference* between the A and B sites of a hexagon cage due to an asymmetric Coulomb field, let us consider some charge at distance $d \gg a$ from the ring center which induces the amplitude

$$u_{\mathrm{H}} \sim \frac{e^2}{\kappa v_{\mathrm{F}}}\frac{a^2}{d^2}\left[\left(\frac{3}{2}\right)^{3/2} - \frac{3}{\sqrt{2}}\right]\left|\begin{Bmatrix}\cos 3\theta_{n_1n_2} \\ \sin 3\theta_{n_1n_2}\end{Bmatrix}\right| \quad \text{for} \quad \begin{Bmatrix}\text{electrons} \\ \text{holes}\end{Bmatrix} \tag{6}$$

at the ring center and at the same time on the H sites outside the considered ring. It depends on the angle $\theta_{n_1n_2}$ of the Wigner crystal orientation: $d = b/\sqrt{3}$ or $d = b$ for interstitials (electrons) or vacancies (holes), respectively. The dimensionless prefactor $e^2/\kappa v_{\mathrm{F}}$ in (6) may be regarded as an "effective fine structure constant," parametrizing the interaction strength [27]. Within a continuum theory, employed from now on for transport properties at $\nu \ll 1$, the nonzero amplitude (6) on the H sites effectively results in a kinetic energy of dopants, associated with the mass

$$m_{\mathrm{eff}} = 1/(v_{\mathrm{F}}a|u_{\mathrm{H}}|), \tag{7}$$

which promotes tunneling through Coulomb barriers to the nearest interstitial or vacancy places at distances $b/\sqrt{3}$ or b, respectively.

As a result, dopants effectively experience a periodic Coulomb potential landscape created by caged Wigner charges. Ignoring correlations between dopants and using path integral methods, the dopant matrix element

$$t_{\mathrm{e/h}} = \Delta e^{-S_0} \tag{8}$$

for hopping between adjacent minima can be estimated within a dilute instanton gas approximation [28]. Equation (8) results from summing over all possible series of independent instanton actions

$$S_0 = 2\sqrt{\frac{e^2m_{\mathrm{eff}}}{\kappa}}\int_{-d/2}^{d/2} dx(x^2 + 3d^2/4)^{-1/4} = C_1\sqrt{\frac{e^2m_{\mathrm{eff}}}{\kappa}}\sqrt{d} \tag{9}$$

for motions in the inverted Coulomb potential $-V(x) = -\frac{2e^2}{\kappa}/\sqrt{x^2 + 3d^2/4}$ by distances d during imaginary times. We assumed that the dominant parts of the Coulomb barrier are created by two charges at distances $\sqrt{3}d/2$ "off the way," which holds true for electron as well as for hole tunneling, and $C_1 \approx 2.096$ is a numerical factor which can be expressed analytically in terms of hypergeometric functions.

Estimates for the ratio Δ of fluctuation determinants in (8) are possible when considering the periodic Coulomb potential $V_0(1 - \cos 2\pi x/d)$ along the tunnel trajectory with $V_0 = \frac{2e^2}{\kappa d}(\frac{2}{\sqrt{3}} - 1)$; then [29]

$$\Delta = \frac{16V_0}{(m_{\mathrm{eff}}V_0)^{1/4}\sqrt{d/2}}. \tag{10}$$

Now we are in the position to estimate the Drude weight $D = e^2 n_{\rm D}/m_{\rm e/h}$ in Eq. (1). Here, $n_{\rm D} = (|\delta\nu|/\nu)n_{\rm e} = 2|\delta\nu|/3^{3/2}a^2$ is the density and the band mass for itinerant electron/hole type dopants takes values of $m_{\rm e/h} = 1/(2t_{\rm e/h}d^2)$, respectively [cf. (8); note that $m_{\rm e/h}$ differs from the kinetic energy mass $m_{\rm eff}$]. Combining Eqs. (6)–(10), our result for the Drude weight becomes

$$D = \frac{e^2 n_{\rm D}}{m_{\rm e/h}} = C_2 \frac{e^2}{\kappa a} \gamma \nu^{-1/8} e^{-S_0} \left| \begin{Bmatrix} \cos 3\theta_{n_1 n_2} \\ \sin 3\theta_{n_1 n_2} \end{Bmatrix} \right|^{1/4} |\delta\nu|, \quad (11)$$

where

$$S_0 = C_3 (\nu\gamma)^{-3/2} \left| \begin{Bmatrix} \cos 3\theta_{n_1 n_2} \\ \sin 3\theta_{n_1 n_2} \end{Bmatrix} \right|^{-1/2}$$

$$\text{for} \quad \begin{Bmatrix} \text{electrons} \\ \text{holes} \end{Bmatrix}, \quad \gamma = \begin{Bmatrix} 3 \\ 1 \end{Bmatrix},$$

and $C_2 = 5.276$ and $C_3 = 20.43$ again are constants that can be expressed analytically.

Qualitatively, this result (11) is sketched in Fig. 2 versus $1/\nu$. Starting from zeros at commensurate fillings $\nu_{n_1 n_2}$, the Drude weight rises linearly with small $|\delta\nu| = |\nu - \nu_{n_1 n_2}|$. Slopes tend to decrease with decreasing filling ν, however, depending on the orientations $\theta_{n_1 n_2}$, they may differ strongly from one zero to the next one. In symmetric cases, $\theta_{n_1 n_2} = \pi/6 + \mathbb{Z}\pi/3$ (electrons) or $\theta_{n_1 n_2} = \mathbb{Z}\pi/3$ (holes), the Drude weight stays constantly zero over a finite range of fillings on one side of $1/\nu_{n_1 n_2}$ (cf. the red arrow in Fig. 2). When the density of the electron type dopants from a lower density $\nu_{n_1 n_2}$ commensurate Wigner crystal equals the density of the hole type dopants from the next higher density $\nu_{n_1' n_2'}$ Wigner crystal, i.e., right in the middle between two adjacent commensurate fillings $\nu_{n_1 n_2}$ and $\nu_{n_1' n_2'}$ (green shaded areas in Fig. 2), according to Landau's rule, a first-order solid to solid phase transition takes place. While sweeping the carrier density, the system has to transform *all* Wigner sites (n_1,n_2) at a crystal orientation $\theta_{n_1 n_2}$ into the next set of Wigner sites (n_1',n_2') at a crystal orientation $\theta_{n_1' n_2'}$. Therefore, at the phase transition, caging should be destroyed entirely and we expect a drastic increase in the Drude weight during the transport measurement, up to values of the order $e^2 n_{\rm e}/m_{\rm eff}$, which exceeds the estimate (11) by a large factor $\sim(\nu/|\delta\nu|)e^{S_0}$.

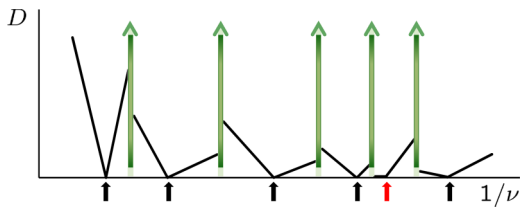

FIG. 2. (Color online) Drude weight D vs inverse flat-band filling $1/\nu$, shown schematically. When $\nu = \nu_{n_1 n_2}$ [cf. Eq. (3)], $D = 0$. Near these zeros (arrows), D rises linearly $\propto|\delta\nu|$ [unless $\theta_{n_1 n_2} = \pi/6 + \mathbb{Z}\pi/3$ or $\theta_{n_1 n_2} = \mathbb{Z}\pi/3$ when D stays constantly zero to the left or right of $\nu_{n_1 n_2}$, respectively (red arrow)]. In the middle, between two adjacent zeros of D (green shaded rectangular areas), the system exhibits a first-order phase transition: There, the Drude weight is expected to rise considerably.

In conclusion, we have studied the Drude weight of flat-band insulators at zero temperature in the presence of long-range Coulomb interactions. A nontrivial function of density is found, exhibiting infinitely many zeros at commensurate fillings, given by Eq. (3). Near those fillings the Drude weight varies linearly with filling. Sweeping the filling under transport conditions, first-order phase transitions of the electron crystal should cause considerably enhanced Drude weights right in the middle between adjacent commensurate fillings.

I am indebted to Reinhold Egger for many inspiring discussions, and acknowledge gratefully sharing aspects of related research with Dario Bercioux and with Daniel Urban. I thank Peter Talkner for valuable feedback on the manuscript, Peter Hänggi for providing fruitful working conditions, and the State of Bavaria for still supporting fundamental research.

[1] E. J. Bergholtz and Z. Liu, Int. J. Mod. Phys. B **27**, 1330017 (2013); S. A. Parameswaran, R. Roy, and S. L. Sondhi, C. R. Phys. **14**, 816 (2013), and references therein.

[2] E. Tang, J.-W. Mei, and X.-G. Wen, Phys. Rev. Lett. **106**, 236802 (2011); K. Sun, Z. Gu, H. Katsura, and S. Das Sarma, *ibid.* **106**, 236803 (2011); T. Neupert, L. Santos, C. Chamon, and C. Mudry, *ibid.* **106**, 236804 (2011); A. M. Läuchli, Z. Liu, E. J. Bergholtz, and R. Moessner, *ibid.* **111**, 126802 (2013).

[3] S. Kourtis, J. W. F. Venderbos, and M. Daghofer, Phys. Rev. B **86**, 235118 (2012).

[4] F. Wang and Y. Ran, Phys. Rev. B **84**, 241103(R) (2011); A. Sterdyniak, C. Repellin, B. A. Bernevig, and N. Regnault, *ibid.* **87**, 205137 (2013); Z. Liu, E. J. Bergholtz, H. Fan, and A. M. Läuchli, Phys. Rev. Lett. **109**, 186805 (2012); S. Kourtis, T. Neupert, C. Chamon, and C. Mudry, *ibid.* **112**, 126806 (2014).

[5] Band flatness cannot be regarded as the limit of band mass m going to infinity, e.g., in a dispersion $\varepsilon_k \propto k^2/2m$, which would yield finite conductance in this limit due to the simultaneously increasing density of states $\propto dk(\varepsilon)/d\varepsilon$ that cancels the effect of decreasing velocity $\propto d\varepsilon_k/dk$.

[6] J. Vidal, R. Mosseri, and B. Douçot, Phys. Rev. Lett. **81**, 5888 (1998).

[7] L. Chen, T. Mazaheri, A. Seidel, and X. Tang, J. Phys. A: Math. Theor. **47**, 152001 (2014).

[8] J. Vidal, B. Douçot, R. Mosseri, and P. Butaud, Phys. Rev. Lett. **85**, 3906 (2000); J. Vidal, P. Butaud, B. Douçot, and R. Mosseri, Phys. Rev. B **64**, 155306 (2001); Z. Gulácsi, A. Kampf, and D. Vollhardt, Phys. Rev. Lett. **99**, 026404 (2007).

[9] C. Wu and S. Das Sarma, Phys. Rev. B **77**, 235107 (2008); S. Takayoshi, H. Katsura, N. Watanabe, and H. Aoki, Phys. Rev. A **88**, 063613 (2013).

[10] See, for example, H. W. Jiang, R. L. Willett, H. L. Stormer, D. C. Tsui, L. N. Pfeiffer, and K. W. West, Phys. Rev. Lett. **65**, 633 (1990).

[11] C.-H. Zhang and Y. N. Joglekar, Phys. Rev. B **75**, 245414 (2007); O. Poplavskyy, M. O. Goerbig, and C. Morais Smith, *ibid.* **80**, 195414 (2009).
[12] B. Tanatar and D. M. Ceperley, Phys. Rev. B **39**, 5005 (1989).
[13] M. Vigh, L. Oroszlány, S. Vajna, P. San-Jose, G. Dávid, J. Cserti, and B. Dóra, Phys. Rev. B **88**, 161413(R) (2013).
[14] R. Chitra and T. Giamarchi, Eur. Phys. J. B **44**, 455 (2005); pinning of Wigner crystals by disorder is beyond the scope of the present work.
[15] W. Kohn, Phys. Rev. **123**, 1242 (1961).
[16] D. Bercioux, D. F. Urban, H. Grabert, and W. Häusler, Phys. Rev. A **80**, 063603 (2009).
[17] For non-time-reversal invariant generalizations, see B. Dóra, I. F. Herbut, and R. Moessner, Phys. Rev. B **90**, 045310 (2014).
[18] D. Green, L. Santos, and C. Chamon, Phys. Rev. B **82**, 075104 (2010).
[19] C. L. Kane and E. J. Mele, Phys. Rev. Lett. **95**, 226801 (2005).
[20] B. Dóra, J. Kailasvuori, and R. Moessner, Phys. Rev. B **84**, 195422 (2011).
[21] B. Sutherland, Phys. Rev. B **34**, 5208 (1986).
[22] G. Meissner, H. Namaizawa, and M. Voss, Phys. Rev. B **13**, 1370 (1976); L. Bonsall and A. A. Maradudin, *ibid.* **15**, 1959 (1977).
[23] M. Kamfor, S. Dusuel, K. P. Schmidt, and J. Vidal, Phys. Rev. B **84**, 153404 (2011).
[24] Unless $|n_1| = |n_2|$ or $n_i = 0$ when only six different pairs (n_1, n_2) exist.
[25] Hard core bosons with short-range interactions on a $\mathcal{T}_3$ lattice seem to realize two domain ground states, see G. Möller and N. R. Cooper, Phys. Rev. Lett. **108**, 045306 (2012).
[26] D. F. Urban, D. Bercioux, M. Wimmer, and W. Häusler, Phys. Rev. B **84**, 115136 (2011).
[27] In suspended graphene, for example, its magnitude is of order $2.2/\kappa$ [I. Sodemann and M. M. Fogler, Phys. Rev. B **86**, 115408 (2012)].
[28] S. Coleman, in *The Whys of Subnuclear Physics*, edited by A. Zichichi, Springer Subnuclear Series Vol. 15 (Springer, Berlin, 1979).
[29] J. Zinn-Justin, Nucl. Phys. B **192**, 125 (1981); Z. Ambroziński, Acta Phys. Pol., B **44**, 1261 (2013).